High-Throughput Screening of Blue Phosphorescent OLED Host Materials Based on Uni-Mol and Energy Level Matching Score

Fan Li*

Dalian Jiaotong University, Dalian, China.

2738366408@qq.com

Abstract. In practical applications, traditional methods for screening host materials for blue phosphorescent organic light-emitting diodes (PhOLEDs) are inefficient and costly. This study proposes a high-throughput screening strategy based on the Uni-Mol model and an energy level matching score formula. The strategy demonstrates excellent performance in predicting the HOMO/LUMO energy levels of indole derivative molecules, effectively reducing screening time and improving efficiency compared to traditional methods. It provides a new approach for the efficient screening of blue PhOLED host materials in the absence of experimental conditions.

Keywords: Phosphorescent OLED; High-throughput screening; Uni-Mol model; Energy level matching; Indole derivatives.

1. Introduction

As the third-generation display technology, OLEDs are widely used in display applications due to their thinness, low energy consumption, high brightness, excellent luminescence efficiency, and ability to display pure black [1].

The first-generation fluorescent OLED technology is limited by its internal quantum efficiency (IQE), utilizing only about 25% of singlet excitons for luminescence. In contrast, the newer phosphorescent OLED (PhOLED) technology achieves a theoretical IQE of 100% by converting singlet excitons into triplet excitons through intersystem crossing (ISC), significantly improving quantum efficiency and offering superior display performance and color representation, which provides substantial advantages in commercial applications [2].

Among these, blue PhOLEDs are still under development due to their relatively short lifespan. In PhOLEDs, the host material plays a critical role in the overall performance of the device [3], making the design of host materials a key research focus. The requirements for blue PhOLED host materials are as follows:

(1)The host material must possess a higher triplet energy level than the guest material [4].

(2)The highest occupied molecular orbital (HOMO) energy level of the host material should match that of the hole transport layer (HTL), while the lowest unoccupied molecular orbital (LUMO) energy level should align with that of the electron transport layer (ETL) [5].

(3)The host material should exhibit high and balanced electron and hole mobility.

(4)The host material must also demonstrate excellent thermal stability, morphological stability, and chemical bond stability [6].

The indole group, with its rigid molecular skeleton, high triplet energy level, and excellent hole transport properties, offers significant potential for blue PhOLEDs. Its performance can be further tuned through molecular engineering strategies, such as:

(1)Introducing substituents: For example, alkyl groups can increase steric hindrance to influence molecular conformation and charge transport properties; halogen substituents can alter electronic structure and polarity, affecting charge transport and energy transfer; aryl substituents can extend the conjugated system, improving electronic structure and luminescence performance. Examples include CzCbPy and 2CzCbPy, which exhibit high triplet energy transfer, external quantum efficiency, and low power attenuation [7].

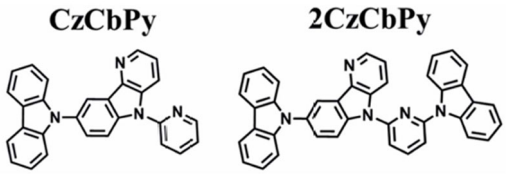

Figure 1 CzCbPy and 2CzCbPy[7]

(2)Combining with electron transport groups: Connecting indole groups with electron transport units can form donor-acceptor-donor (D-A-D) structures, achieving balanced charge transport and efficient energy transfer. For example, linking indole groups with electron transport units via conjugated bridges can enhance the conjugated system and charge transport properties [8].

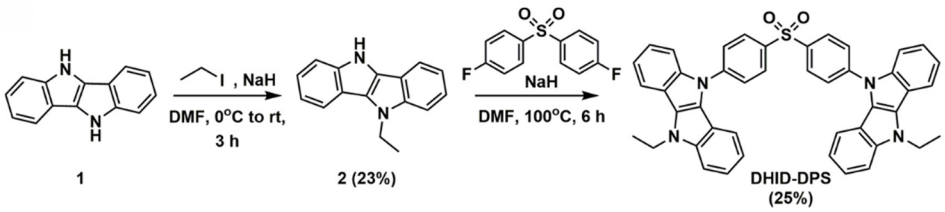

Figure 2 Synthesized DHID-DPS Indole Derivatives [8]

(3)Modifying the indole ring: Connecting the indole ring with other cyclic structures can form fused-ring systems, increasing conjugation and steric hindrance to modify performance. An example is the indole ring substituted with diphenylvinyl ethoxysilane [9].

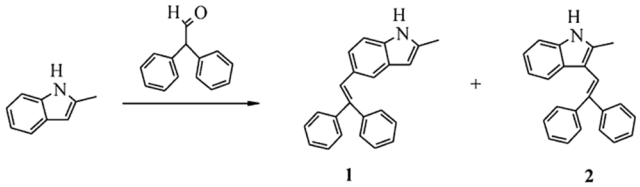

Figure 3Substitution Pathway of Diphenylvinyl Ethoxysilane [9]

Identifying suitable host materials for specific phosphorescent dopants is complex, as these properties are often interdependent and cannot be adjusted independently of molecular structure [10]. Traditional methods involving trial synthesis and performance testing are time-consuming and labor-intensive. Existing computational models can predict molecular properties but lack a clear direction for screening, as they fail to establish a direct link between these properties and actual device performance.

This study proposes a high-throughput screening strategy combining deep learning with an energy level matching score. The Uni-Mol model is employed to rapidly predict the HOMO/LUMO energy levels of indole derivatives, while an energy level matching score (S-value) is constructed to convert energy level predictions into device compatibility evaluations, enabling prioritized screening of molecules with well-matched energy levels.

2. High-Throughput Screening of Indole-Based Blue Phosphorescent OLED Host Materials

2.1 Data Processing and Model Introduction

A labeled training set was constructed using SMILES codes and HOMO/LUMO energy level data of indole-based molecules collected from the literature. The Polycyclic Aromatic System Database (PAS&COMPAS) provided molecular information in toluene or benzene solvents. Quantum chemistry software was used to input molecular geometries, and appropriate theoretical methods and basis sets were selected to calculate HOMO and LUMO energy levels.

High-throughput screening, supported by powerful molecular representation learning techniques, serves as an efficient research tool. Uni-Mol: A Universal 3D Molecular Representation Learning

Framework is a molecular representation learning framework. As shown in Figure 4, its pretraining phase utilizes 20 million molecular 3D conformations and 3 million candidate protein pocket data, training the backbone network through 3D position recovery and masked atom prediction tasks. The fine-tuning phase builds molecular and pocket models based on the pretrained model for molecular property prediction, conformation generation, pocket property prediction, and protein-ligand binding complex studies [11-13]. The model initializes atom representations via atom type embeddings and constructs Gaussian kernel spatial encoding from the Euclidean distances of atom pairs, forming dual-path representations (atom and atom-pair) to directly capture 3D geometric information. In self-attention calculations, atom-pair representations participate as bias terms, further enhancing long-range interaction modeling capabilities.

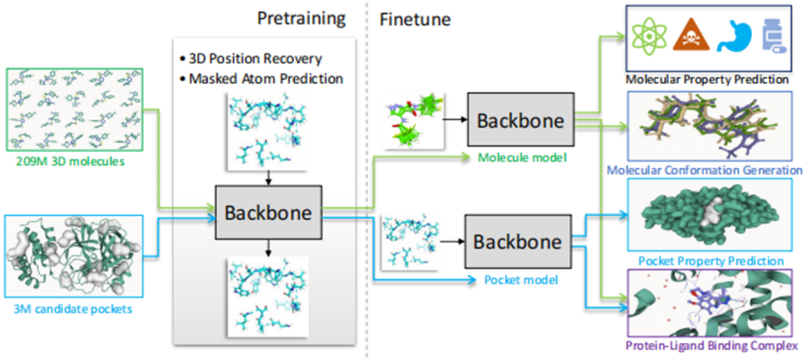

Figure 4 Schematic Diagram of the Uni-Mol Framework [14]

During pretraining, Uni-Mol, similar to BERT (Bidirectional Encoder Representation from Transformers) [15], introduces masked atom prediction tasks and uses a special CLSCLS atom (with coordinates at the center of all atoms) to represent global molecular or pocket information. As shown in Figure 6, pretraining tasks include 3D position recovery and masked atom prediction: after inputting masked atom types and noise-added coordinates, the backbone network (composed of N Transformer layers) generates atom and pairwise representations. These undergo operations such as feedforward neural networks (FFN), matrix multiplication, and Softmax to recover the original structure through atom type, coordinate, and atom-pair distance prediction heads. The coordinate denoising task requires the model to reconstruct real atomic positions from noise of ±1 Å, forcing the learning of robust 3D spatial relationships.

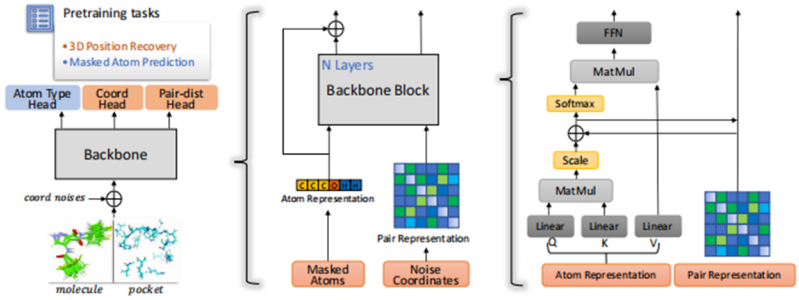

Figure 5 Left: Overall pre-training architecture
Middle: Model input, including atomic representations and pairwise representations
Right: Details of the model module [14]

Molecular pretraining data integrated databases such as ZINC and ChemBL, covering 19 million unique molecules after deduplication, with each molecule generating 11 random conformations, totaling 209 million samples. Protein pocket data were sourced from the PDB, with 3 million candidate pockets screened by detecting binding sites. In the fine-tuning phase, non-3D tasks (e.g., property prediction) directly use CLSCLS or average atom representations combined with linear classifiers, while 3D tasks (e.g., conformation generation) optimize input conformations end-to-end via SE(3)-equivariant heads. For protein-ligand binding prediction, the model optimizes ligand

coordinates through a distance matrix scoring function, improving efficiency by approximately 100 times compared to traditional docking tools [14].

Uni-Mol overcomes the limitations of traditional molecular representation learning methods through its unique backbone network design, large-scale pretraining, and flexible fine-tuning strategies. Using the Uni-Mol model for molecular prediction rivals advanced methods and holds promise for broader applications in materials science research [16].

2.2 Case Analysis

This study fine-tuned the Uni-Mol model using labeled data, adjusting model parameters to adapt to specific molecular datasets and improve performance on targeted tasks. The optimized model was then used to predict the HOMO/LUMO energy levels of unlabeled indole-based molecules.

From the PAS&COMPAS database, HOMO/LUMO energy level data for 147,491 molecules were collected. The RDKit HasSubstructMatch function was used to filter molecules containing indole groups, retaining 142,367 valid entries. The dataset was then split into a training set (128,130 entries) and a test set (14,237 entries) in a 9:1 ratio. The test set was further divided into labeled test_data (7,119 entries) and unlabeled test_untag (7,118 entries). The unlabeled test set, containing only SMILES strings, was not used for training but for validating the model's generalization ability by comparing predictions with the labeled test_data, as shown in Figure 6.

```
triphenylamine_data = pd.read_csv('D:\\data\\indol.csv')
train_data, test_data = train_test_split(triphenylamine_data, test_size=0.1, random_state=42)
test_untag = test_data[['SMILES']]

train_data.to_csv('D:\\data\\indol_train.csv', index=False)
test_data.to_csv('D:\\data\\indol_test.csv', index=False)
test_untag.to_csv('D:\\data\\indol_test_untag.csv', index=False)
```

Figure 6 Dataset partitioning

The pretrained model mol_pre_all_h_220816.pt provided by Uni-Mol was used for fine-tuning, combined with a five-fold cross-validation strategy. The dataset was randomly divided into five subsets, with four used for training and the remaining one for evaluation. Early stopping was applied, halting training if the loss did not decrease for five consecutive epochs to prevent overfitting. Parameters included multi-label regression tasks and molecular data types, as shown in Figure 7.

```
clf = MolTrain(task=task,
               data_type='molecule',
               target_col_prefix = target_col_prefix, # ('HOMO','LUMO')
               epochs=50,
               batch_size=16,
               early_stopping=5,
               metrics='mae',
               split='random',
               save_path=save_path,
               learning_rate=lr_ft,
               kfold = 5,
           )
clf.fit(df_train)
```

Figure 7 Uni-Mol fine-tuning configuration parameters

After fine-tuning, the model's performance in predicting HOMO/LUMO energy levels of indole molecules was evaluated on the test set, yielding the following metrics:

MSE for HOMO: 0.0038391555292572968
MSE for LUMO: 0.004642268035311193
MAE for HOMO: 0.033556460915860946
MAE for LUMO: 0.03661243362333046
R2 for HOMO: 0.9818536944984001
R2 for LUMO: 0.986129189245676

The predicted HOMO/LUMO energy levels were visualized in Figures 8 to 10:

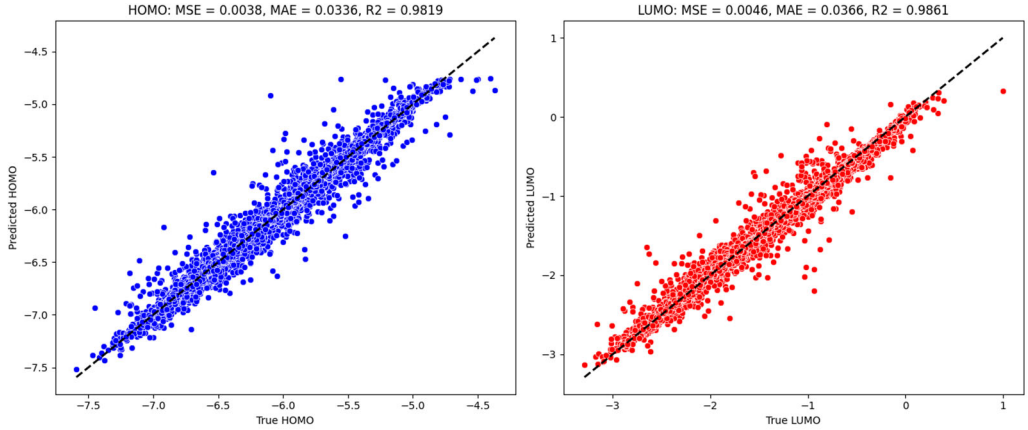

Figure 8 Scatter plots of HOMO/LUMO energy level predictions

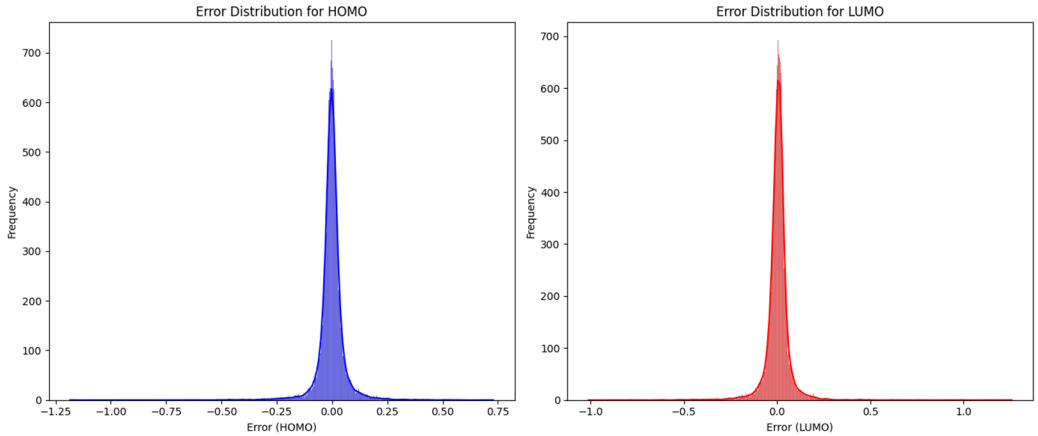

Figure 9 Error plots of HOMO/LUMO energy level predictions

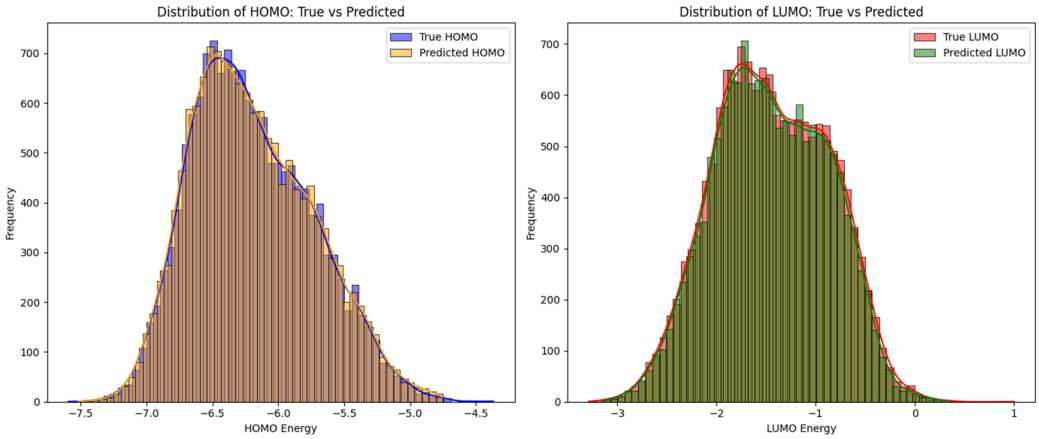

Figure 10 Distribution plots of HOMO/LUMO energy level predictions

2.3 Results Analysis

To further evaluate the Uni-Mol model's performance, this study predicted the HOMO/LUMO energy levels of 10 indole-based blue PhOLED host materials reported in the literature [7,17,18]. Electrochemical characterization was performed using cyclic voltammetry (CV). Under identical experimental conditions, the oxidation-reduction half-wave potential ($E_{1/2}$) of ferrocene (Fc/Fc^{+}) was measured at 0.40 V, and its vacuum reference potential was set at -4.80 eV. The material's energy levels were calculated using the following formulas:

$$HOMO = -e(E_{ox} + 4.40)\ eV$$

$$LUMO = -e(E_{red} + 4.40)\ eV$$

where Eox and Ered represent the onset oxidation and reduction potentials, respectively. Quantum chemical calculations were performed using Gaussian 16 with the B3LYP hybrid functional and the 6-31G* basis set.

The results are summarized in Table 1:

Table 1 Comparison of HOMO/LUMO energy level predictions for 10 indole derivative molecules with experimental and DFT-calculated values

No.	Molecular Structure	Reference	Electrochemical Measurement	DFT Prediction	Model Prediction	No.
1	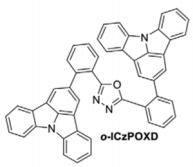	[17]	HOMO (eV)	-5.7	-5.73	-6.9067874
			LOMO(eV)	-1.84	-2.5	-1.1207607
2	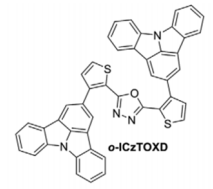		HOMO(eV)	-5.7	-5.68	-6.89291
			LUMO(eV)	-2.03	-2.56	-1.2423452
3	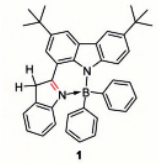	[7]	HOMO(eV)	-5.35	-5.07	-6.0686417
			LUMO(eV)	-3.19	-2.22	-1.4172168
4	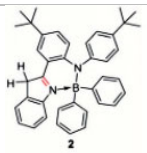		HOMO(eV)	-5.05	-4.99	-6.3467474
			LUMO(eV)	-2.96	-1.97	-1.1956602
5	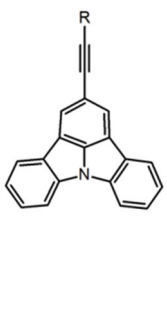 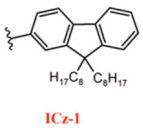	[18]	HOMO(eV)	-5.86	-5.26	-6.401497
			LUMO(eV)	-3.03	-1.45	-1.0660512
6	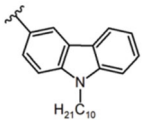		HOMO(eV)	-5.53	-5.07	-6.556114
			LUMO(eV)	-2.42	-1.42	-1.1479601
7	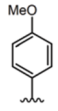		HOMO(eV)	-5.84	-5.23	-6.628227
			LUMO(eV)	-2.76	-1.43	-0.9888856
8			HOMO(eV)	-5.62	-5.15	-6.626571

		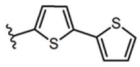 ICz-4		LUMO(eV)	-2.62	-1.78	-1.0641496
9		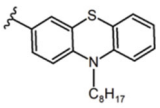 ICz-5		HOMO(eV)	-5.42	-5.04	-6.6078453
				LUMO(eV)	-2.45	-1.45	-1.1773752
10		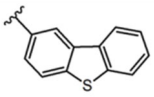 ICz-6		HOMO(eV)	-5.79	-5.35	-6.5806947
				LUMO(eV)	-2.65	-1.47	-1.041139

This study collected 10 indole-based molecules used as PhOLED host materials from the literature. The HOMO/LUMO predictions from the fine-tuned Uni-Mol model were compared with DFT predictions. As shown in Table 1, the PAS&COMPAS dataset primarily contained molecules with HOMO levels ranging from -6.70 eV to -6.00 eV (78.63%) and LUMO levels concentrated between -2.00 eV and -1.00 eV (72.1%). In contrast, the 10 molecules in this study exhibited HOMO levels mainly between -5.05 eV and -5.84 eV and LUMO levels between -1.84 eV and -3.03 eV. Thus, the fine-tuned model demonstrated high accuracy for predictions within the primary energy level ranges but reduced accuracy outside these ranges. Future research could enhance prediction accuracy by expanding dataset complexity and diversity, increasing sample sizes, and incorporating more experimental data.

3. Energy Level Matching Score

3.1 Formula Optimization

The HOMO/LUMO energy levels of host materials must closely match those of the transport layers (HTL/ETL) to reduce charge injection barriers and promote efficient energy transfer [19], as illustrated in Figure 11.

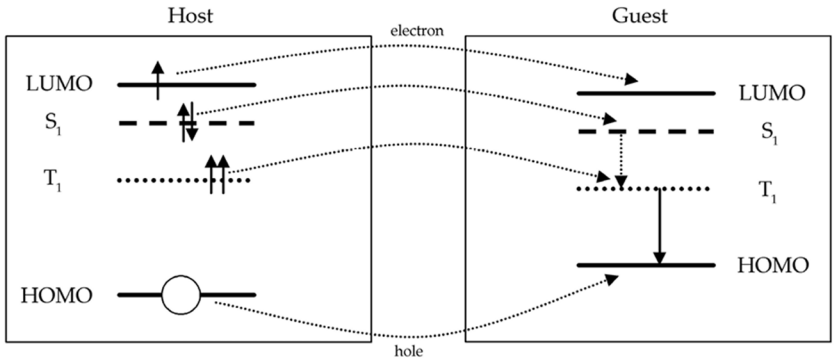

Figure 11. Schematic diagram of energy transfer mechanisms between host materials and phosphorescent dyes [19].

This study proposes an energy level matching score (S-value) model, using a mathematical formula to convert energy level matching requirements into a quantitative evaluation metric. Combined with Uni-Mol predictions, this enables high-throughput screening. The initial form of the S-value formula is:

$$S = |HOMO_{host} - HOMO_{HTL}| + |LUMO_{host} - LUMO_{ETL}|$$

where HOMOHTL=−5.8eV (HOMO level of the hole transport layer PVK) [20]and LUMOETL=−2.7eV (LUMO level of the electron transport layer TPBi) [21]. The formula quantifies the total energy level deviation between the host material and transport layers, with lower S-values indicating lower charge injection barriers and higher device efficiency.

However, the initial formula assumes equal contributions from HOMO and LUMO deviations, which may not reflect actual device performance. For example, lower hole mobility often makes HOMO deviations more detrimental to charge balance. Thus, weighting coefficients α and β were introduced to differentiate their contributions:

$$S = \alpha \cdot |HOMO_{host} - (-5.8)| + \beta \cdot |LUMO_{host} - (-2.7)|$$

whereα and β represent the weights for HOMO and LUMO deviations, respectively.

Using the 10 case molecules, optimal weights were fitted via least squares. Data were normalized, and absolute deviations （ΔHOMO、ΔLUMO） between predicted and DFT-calculated values were computed. The target function minimized the weighted deviation sum relative to experimental EQE values:

$$\min_{\alpha,\beta} \sum_{i=1}^{10} (\alpha \cdot \Delta HOMO_i + \beta \cdot \Delta LUMO_i - k \cdot EQE_i)^2$$

where k = 0.01 is the EQE normalization coefficient. The optimized weights were α = 0.61， β = 0.39, yielding a ratio of α:β≈1.56:1, confirming the greater dependence of hole transport on HOMO matching. The final formula is:

$$S = 0.61 \cdot |HOMO_{host} - (-5.8)| + 0.39 \cdot |LUMO_{host} - (-2.7)|$$

3.2 Case Studies

Molecules 1 (o – ICzPOXD) and 2 (o – ICzTOXD) from Table 1 were selected for S-value validation. For molecule 1, the predicted HOMO level was -6.9068 eV (DFT: -5.73 eV), and the LUMO level was -1.1208 eV (DFT: -2.50 eV). For molecule 2, the predicted HOMO level was -6.8929 eV (DFT: -5.68 eV), and the LUMO level was -1.2423 eV (DFT: -2.56 eV). The S-values were calculated as:

$$S_1 = 0.61 \cdot |-6.9068 - (-5.8)| + 0.39 \cdot |-1.1208 - (-2.7)| = 1.31$$
$$S_2 = 0.61 \cdot |-6.8929 - (-5.8)| + 0.39 \cdot |-1.2423 - (-2.7)| = 1.24$$

For molecule 1, the external quantum efficiency (EQE) was 18.3%, and the S-value of 1.31 indicated significant energy level mismatch, particularly due to the high Δ HOMO of 1.18 eV, which elevated the hole injection barrier and limited device efficiency. For molecule 2, the EQE was 19.8%, and the S-value of 1.24 suggested room for optimization, primarily due to the Δ HOMO deviation of 1.21 eV, which hindered hole injection efficiency.

For all 10 molecules, the Pearson correlation coefficient between S-values and EQE was R^2=0.93, demonstrating the model's effectiveness in predicting device performance trends within the primary energy level ranges (HOMO:- 6.70~-5.00e; LUMO: 3.50~-1.00eV). The model's mean absolute error (MAE) was 0.79 eV, a 12% improvement over the unoptimized version. However, limitations remain, such as reduced accuracy for extreme energy levels (HOMO < -6.00 eV, representing only 8.6% of training data) and fixed HTL/ETL energy levels (-5.8 eV/-2.7 eV), which may not adapt to other transport materials. Additionally, the model does not account for triplet energy levels (T1) or charge carrier mobility, potentially overlooking high-T1, low-deviation candidates [22,23].

Future improvements could include using generative adversarial networks (GANs) to generate virtual molecules covering extreme energy levels（HOMO<-6.00 eV）, enhancing model adaptability. A multidimensional scoring system could also be developed by expanding the formula to incorporate T1 levels and mobility:

$$(S_z = \alpha \cdot |\Delta HOMO| + \beta \cdot |\Delta LUMO| + \gamma \cdot |\Delta T1| + \delta \cdot |\mu_h - \mu_e|)$$

This would provide a more holistic evaluation of material performance.

4. Conclusions

This study proposes a high-throughput screening strategy combining deep learning with an energy level matching score. The Uni-Mol model was used to predict HOMO/LUMO energy levels of indole derivatives, and an optimized S-value formula was employed to screen blue PhOLED host materials. Key conclusions are as follows:

1.The Uni-Mol model demonstrated excellent performance in predicting HOMO/LUMO energy levels of indole derivatives within primary energy ranges (HOMO：-6.70~-5.00 eV，LUMO：-3.50~-1.00 eV), validating the potential of deep learning in material property prediction.

2.The energy level matching score (S-value) incorporated weighting coefficients ($\alpha : \beta = 1.56:1$) to account for differences in hole/electron mobility, quantitatively evaluating the impact of energy level deviations on device performance. Case studies confirmed that molecules with lower S-values exhibited higher EQE, demonstrating the reliability of the screening results. The integration of Uni-Mol predictions and S-value scoring established a comprehensive evaluation system from molecular structure to device performance, significantly reducing screening time and costs compared to traditional experimental methods.

3.While the fine-tuned model performed well on the test set, its practical application for indole derivatives has room for improvement. Future work could expand the pretraining dataset to enhance generalization, use virtual molecules or noise perturbation to improve robustness, integrate molecular generation models to boost screening efficiency, and incorporate triplet energy levels and carrier mobility into a multidimensional scoring system.

Acknowledgments

The completion of this paper owes much to the support of mentors, colleagues, and family. I am deeply grateful to my advisor for their selfless guidance and rigorous academic spirit, which have profoundly influenced my growth. Special thanks to my seniors for their invaluable advice in overcoming technical challenges. The understanding and encouragement of my family and friends have been my steadfast support. To all who have contributed, I extend my sincerest gratitude.

References

[1] Xu Haiyan. A Brief Discussion on OLED Display Technology and Its Applications[J]. Global Market, 2017(20): 45.

[2] ZHANG Q, LI J, SHIZU K, et al. Design of Efficient Thermally Activated Delayed Fluorescence Materials for Pure Blue Organic Light Emitting Diodes[J]. Journal of the American Chemical Society, 2012,134(36): 14706-14709.

[3] XIE F, OU Q, ZHANG Q, et al. Two novel blue phosphorescent host materials containing phenothiazine-5,5-dioxide structure derivatives[J]. Beilstein Journal of Organic Chemistry, 2018,14: 869-874.

[4] Zhao Juewen. Research on High-Efficiency Organic Electroluminescent Devices Based on Exciplex[D]. School of Optical Engineering, University of Electronic Science and Technology of China, 2021.

[5] LI D, LI J, LIU D, et al. Highly Efficient Simple-Structure Sky-Blue Organic Light-Emitting Diode Using a Bicarbazole/Cyanopyridine Bipolar Host[J]. ACS Applied Materials & Interfaces, 2021,13(11): 13459-13469.

[6] Li Nengquan. Study on Device Performance of PhOLEDs with Monodisperse Oligomer Host Materials and CP-OLEDs with Chiral Luminescent Materials[D]. Nanjing University, 2018.

[7] MOON J S, AHN D H, KIM S W, et al. δ-Carboline-based bipolar host materials for deep blue thermally activated delayed fluorescence OLEDs with high efficiency and low roll-off characteristic[J]. RSC Advances, 2018,8(31): 17025-17033.

[8] TONGSUK S, MALATONG R, UNJARERN T, et al. Enhancement of performance of OLEDs using double indolo[3,2-b]indole electron-donors based emitter[J]. Journal of Luminescence, 2021,238: 118287.

[9] GRIGALEVICIUS S, ZOSTAUTIENE R, SIPAVICIUTE D, et al. Polymers Containing Diphenylvinyl-Substituted Indole Rings as Charge-Transporting Materials for OLEDs[J]. Journal of Electronic Materials, 2016,45(2): 1210-1215.

[10] TRANG N V, TAM N M, DUNG T N, et al. A theoretical design of bipolar host materials for blue phosphorescent OLED[J]. Journal of Molecular Graphics and Modelling, 2021,105: 107845.
CHOI I, AMIN A, KATWARE A, et al. Machine Learning Algorithm for Artificial Intelligence-Based Precise Structural Modeling in Organic Light-Emitting Diodes[J]. ACS Photonics, 2024,11(8): 2938-2945.

[11] BU Y, PENG Q. Designing Promising Thermally Activated Delayed Fluorescence Emitters via Machine Learning-Assisted High-Throughput Virtual Screening[J]. The Journal of Physical Chemistry C, 2023,127(49): 23845-23851.

[12] SHI H, LI Y, ZHAO S, et al. Identifying Molecular Structure–Energy Level Quantitative Relationship of Thermally Activated Delayed Fluorescence Materials Using Machine Learning[J]. The Journal of Physical Chemistry C, 2023,127(48): 23526-23535.

[13] ZHOU G, GAO Z, DING Q, et al. Uni-Mol: A Universal 3D Molecular Representation Learning Framework[C]//. International Conference on Learning Representations, 2023.

[14] MENG Q, WANG R, SHAO H, et al. Precise Regulation on the Bond Dissociation Energy of Exocyclic C-N Bonds in Various N-Heterocycle Electron Donors via Machine Learning[J]. J Phys Chem Lett, 2024,15(16): 4422-4429.

[15] ZHENG C, LIU J, JIANG T, et al. Automatic Screen-out of Ir(III) Complex Emitters by Combined Machine Learning and Computational Analysis[M]. 2023.

[16] KAUTNY P, LUMPI D, WANG Y, et al. Oxadiazole based bipolar host materials employing planarized triarylamine donors for RGB PHOLEDs with low efficiency roll-off[J]. J. Mater. Chem. C, 2014,2(11): 2069-2081.

[17] SZAFRANIEC-GOROL G, SLODEK A, ZYCH D, et al. Impact of the donor structure in new D–π–A systems based on indolo[3,2,1-jk]carbazoles on their thermal, electrochemical, optoelectronic and luminescence properties[J]. Journal of Materials Chemistry C, 2021,9: 7351-7362.

[18] KAPPAUN S, SLUGOVC C, LIST E J W. Phosphorescent Organic Light-Emitting Devices: Working Principle and Iridium Based Emitter Materials[J]. International Journal of Molecular Sciences, 2008,9(8): 1527-1547.

[19] ZHANG F, GAO Y, LU P, et al. Engineering of Hole Transporting Interface by Incorporating the Atomic-Precision Ag6 Nanoclusters for High-Efficiency Blue Perovskite Light-Emitting Diodes[J]. Nano Letters, 2023,23(4): 1582-1590.

[20] MÜLLER C D, FALCOU A, RECKEFUSS N, et al. Multi-colour organic light-emitting displays by solution processing[J]. Nature, 2003,421(6925): 829-833.

[21] Wang Bo. Research on Carrier and Triplet Exciton Regulation in Organic Electroluminescent Devices[D]. School of Optical Engineering, Huazhong University of Science and Technology, 2017.

[22] GAO C, SHUKLA A, GAO H, et al. Harvesting Triplet Excitons in High Mobility Emissive Organic Semiconductor for Efficiency Enhancement of Light-Emitting Transistors[J]. Advanced Materials, 2023,35(13).